

FIRE\_CCI

**Special Case Study on Fires in Indonesia and El Niño:  
Object-based burned area detection and related fire emission  
estimations based on Sentinel-1 data**

D1

Algorithm Theoretical Basis Document

Prepared for European Space Agency (ESA-ESRIN)

In response to ESRIN/Contract No. 4000115006/15/I\_NB



December 2016

## Revision History

<b>Deliverable</b>	<b>D1</b>		
<b>Work Package</b>	Phase I		
<b>Due date</b>	KO+7		
<b>Authors</b>	Sandra Lohberger, Matthias Stängel, Florian Siegert		
<b>Distribution</b>			
<b>Reason for change</b>		CCI-FIRE-EOPS-MM-16-0139	
<b>Issue</b>			
<b>Revision</b>	1		
<b>Date</b>		15 December 2016	
<b>Release</b>	2		
<b>Version</b>	01		



# Table of Contents

1	General overview.....	5
2	Introduction .....	5
3	General description of the project area .....	7
4	Datasets .....	8
4.1	Burned area detection .....	8
4.1.1	Sentinel-1.....	8
4.1.2	MODIS hotspots.....	10
4.1.3	TRMM.....	10
4.1.4	SRTM .....	10
4.1.5	PALSAR-2 .....	10
4.1.6	Water bodies .....	10
4.1.7	Sentinel-2.....	11
4.1.8	Field data .....	11
4.2	Fire Emission estimation .....	11
4.2.1	ESA GlobBiomass map .....	11
4.2.2	MoEF land cover .....	12
4.2.3	ESA CCI land cover.....	12
4.2.4	Landsat-8 .....	12
4.2.5	SPOT-5.....	12
4.2.6	Wetlands International peat layer.....	12
5	Methodology.....	12
5.1	Burned area detection .....	12
5.1.1	Sentinel-1 processing .....	12
5.1.2	Sentinel-2 and Landsat-8 pre-processing .....	14
5.1.3	Object based burned area classification approach.....	14
5.1.4	ALOS-2 cross comparison .....	14
5.2	Reference land cover classification.....	15
5.3	Emission estimation.....	16
5.3.1	Vegetation fire emissions.....	16
5.3.2	Peat fire emissions .....	19
5.4	Strengths, limitations and weakness of the developed approach .....	19
6	Products.....	19
7	References .....	19

## List of Tables

Table 1: Number of MODIS Hotspots in the three regions between 01.07.2015 and 31.10.2015 and the fractional number of hotspots falling within slopes $>15^\circ$ .....	8
Table 2: Sentinel-1A data used for burned area mapping of 2015 showing the different characteristics (polarization, orbit and acquisition dates).....	8
Table 3: Used datasets for fire emission estimation. ....	11
Table 4: Acquisition dates for Sentinel-1 and PALSAR-2 cross comparison. ....	14
Table 5: Emission factors used for each land cover class for the different land cover classifications. The values are based on extensive LiDAR analyses conducted within the GIZ FORCLIME and BIOCLOME projects. ....	17

## List of Figures

Figure 1: MODIS imagery and hotspot data from 24 September 2015 showing that thick haze from wildfires on Borneo. ....	6
Figure 2: The project area covering Sumatra, Kalimantan and Papua. The bar chart depicts the total area of each region with excluded areas (slope $> 15^\circ$ ). ....	7
Figure 3: Overview of the different orbits for each region showing the internal orbit number listed in Table 2.....	9
Figure 4: Available pre- and post-fire acquisitions (coloured bars) for the Kalimantan region are shown with monthly TRMM precipitation data (blue bars, right Y-Axis) and number of MODIS hotspots (red line, left Y-Axis).....	10
Figure 5: Pre-processing workflow.....	13
Figure 6: Location of the 100.000 km <sup>2</sup> site where the reference land cover classification was conducted. ....	15
Figure 7: The left image represents the stratify and multiply approach, where a land cover classification with assigned emission factors is used to calculate emissions of burned areas. On the right the continuous approach is depicted, where each pixel holds different emission factors based on the biomass of the vegetation. ....	17

# 1 General overview

Indonesia's invaluable tropical forests are home to many endangered species, comprise high biodiversity and store huge amounts of carbon. However, these forests are threatened by wild fires each year during the dry season. A very severe El Niño hit Indonesia in 2015 and resulted in an extreme drought. Consequences were vast disastrous forest and peat fires.

The aim of this project is to estimate damage caused by these fires in Indonesia 2015/2016 using Sentinel-1 imagery. Comprehensive burned area maps derived from Sentinel-1 imagery are created for Indonesia's three largest islands, namely Sumatra (480,000 km<sup>2</sup>), Kalimantan (536,000 km<sup>2</sup>) (part of the island Borneo) and West-Papua (460,000 km<sup>2</sup>) for the dry season of 2015 and 2016. The resulting burned area maps are validated using multispectral Sentinel-2 and Landsat-8 data of acceptable cloud coverage as well as using field information collected in alliance with GIZ in Sumatra. Fire emission estimates are then derived for the study period using existing carbon stock and land cover maps with corresponding emission factors.

# 2 Introduction

Vast and disastrous forest and peat fires were raging across Indonesia in 2015 putting Indonesia on track to be one of the world's largest carbon emitters this year. Especially peat fires are smouldering underground and produce thick haze drifting to neighbouring countries Malaysia, Singapore and Thailand. The thick haze causes not only economic harm but also health issues caused by the pollution: The Pollutant Standards Index (PSI) is an air quality index which broadly exceeded values of 300 which represent "hazardous" air quality. In Central Kalimantan, an alarming PSI value of 1,801 was recorded on 1st October 2015. It is assumed that the fires are mostly started deliberately and illegally for large-scale plantation development for pulpwood and oil palm. The drainage of peatland areas increases the susceptibility to fires which is further enhanced by strong El Niño episodes causing a prolonged drought period. In 2015, the region was experiencing a very strong El Niño climate phenomenon. Recent estimates from the Global Emission Fire Database indicate that Indonesia's fire emissions from 2015 are estimated at 1.75 Gt of carbon [1].

These estimates contain a substantial amount of uncertainty related to the complex fire situation and the fact that they are based on fire detections derived from MODIS. NASA's two MODIS satellites Aqua and Terra make active fire data available every day by applying a fire and thermal anomalies algorithm [2]. Thermal anomalies or active fires represent the centre of a 1 km<sup>2</sup> pixel containing one or more fires within the pixel. This is the most basic fire product in which active fires and other thermal anomalies, such as volcanoes, are identified. However, thick haze and clouds prevent the detection of active fires which in turn result in substantial underestimation of fire events (see Figure 1). Fires were only detected in areas where the blanket of haze was thin enough.

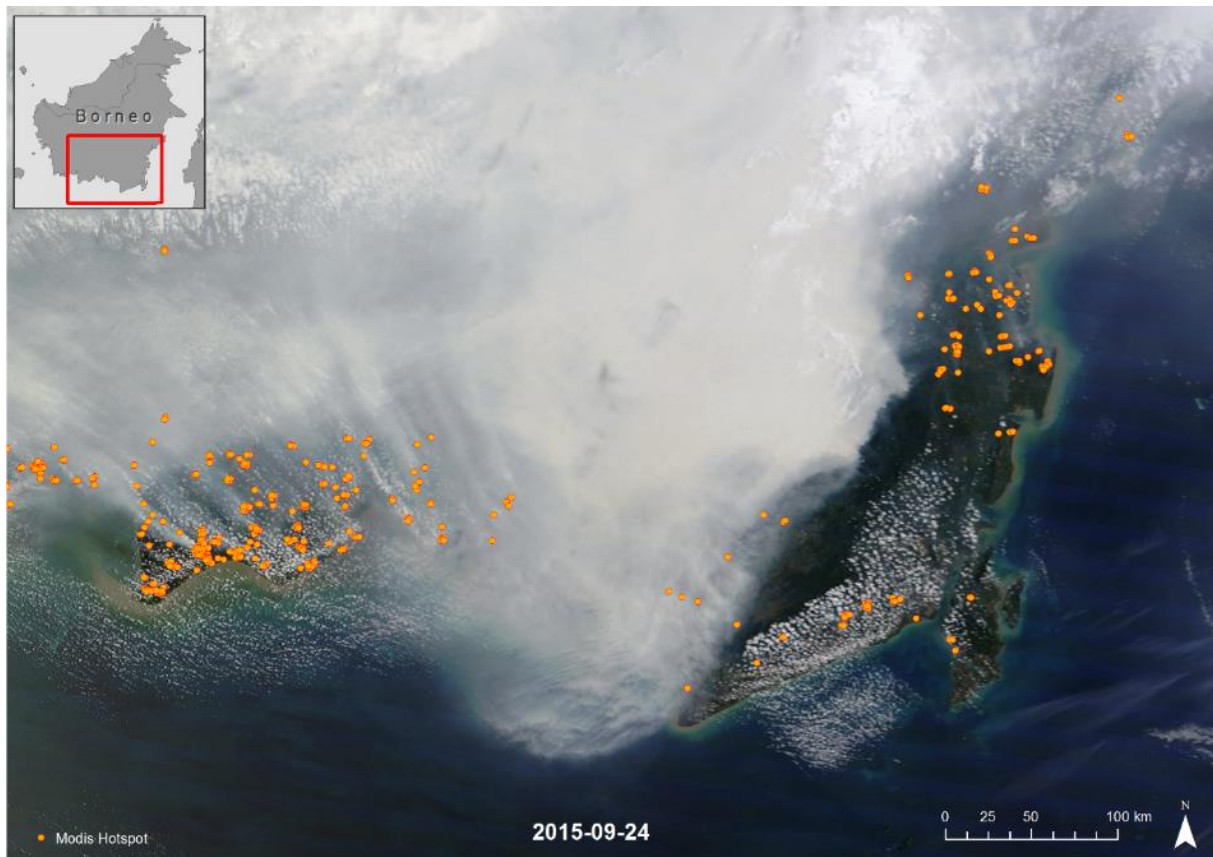


Figure 1: MODIS imagery and hotspot data from 24 September 2015 showing that thick haze from wildfires on Borneo.

In an attempt to monitor and contain these fires, ground teams assess the extent and intensity of fire damage. Nevertheless, their reports describe difficulties in measuring impacts onsite and underline the need for additional management techniques. In contrast, remote sensing approaches appear to present a viable solution for fire management. The European C-band SAR satellite Sentinel-1 can penetrate thick haze and detect damage caused by recent fires on the ground. Similarly, valuable multispectral imagery of regions before and after fires can be acquired by Sentinel-2, in order to complete the time series analyses.

The aim of this project is to estimate the damage caused by the fire catastrophe 2015 in Indonesia and related fire emissions as well as for the year 2016. Comprehensive burned area maps derived from Sentinel-1 imagery are created for fire prone areas in the three largest islands of Indonesia (Sumatra, Kalimantan and West-Papua). An object-based classification approach for Sentinel-1 was developed which detects the disturbance between two time steps, one before and one after the fire. The resulting burned area maps are then validated on one hand by using Sentinel-2 and Landsat-8 data of acceptable cloud coverage, and on the other hand based on in-situ data collected in alliance with the GIZ (German Corporation for International Cooperation) for Sumatra. Previous work has shown that burn scars can be identified with high accuracy in Landsat or Sentinel-2 imagery using an object-based classification approach [3]. Emission estimates will be derived for the study period, using methodologies developed for and presented in Borneo's GlobBiomass study or existing land cover maps such as CCI Land Cover or Indonesian Ministry of Environment and Forestry (MoEF) land cover maps with corresponding emission factors. These existing land cover maps are cross-compared with a separately produced land cover map on a 100.000 km<sup>2</sup> study site. The method presented here will also be assessed against similar approaches being developed for Africa, to determine the best technique to apply given data with high spatial resolution and persistent cloud cover.

### 3 General description of the project area

The project area covers three regions in Indonesia, Sumatra (473,481 km<sup>2</sup>), Kalimantan (536,385 km<sup>2</sup>) (part of the island Borneo) and West-Papua (319,036 km<sup>2</sup>) with a total area of more than 1,329,000 km<sup>2</sup>. The climate is defined as tropical having seasonal climatic characteristics with a rainy season from November until March and a dry season from June to October. Additionally to this seasonal climatic effect, the intermittent El Niño phenomena leads to even dryer conditions during the dry season and to an increase of the potential of fires. Each year during the dry season Indonesia is struck by numerous fire events which drastically decrease forested areas. The number of fires rises tremendously during an intense El Niño period as occurred for example in 2015. Additionally to the high carbon stocks of tropical forests, large areas are covered by peat which are huge carbon sinks and emit disproportionate amounts of carbon.

Indonesia has a long story of fires, devastating entire regions whereas the fires in 1997/1998 are probably the most well-known due to their intensity. Fires in Indonesia are mostly intentional to clear land for cultivation via the fast and cheap "slash and burn" method mostly in flat regions. However, Indonesia has great mountain ranges where only a small amount of fires occur.

In this project, high slopes (>15°) were excluded for burned area mapping due to relief displacement effects occurring in SAR data in steep terrain. In total, 304,855 km<sup>2</sup> were masked out for burned area analysis which is app. 23% of the project area which in turn comprise less than 2% of all active fire detections by MODIS hotspots (Figure 2 and Table 1).

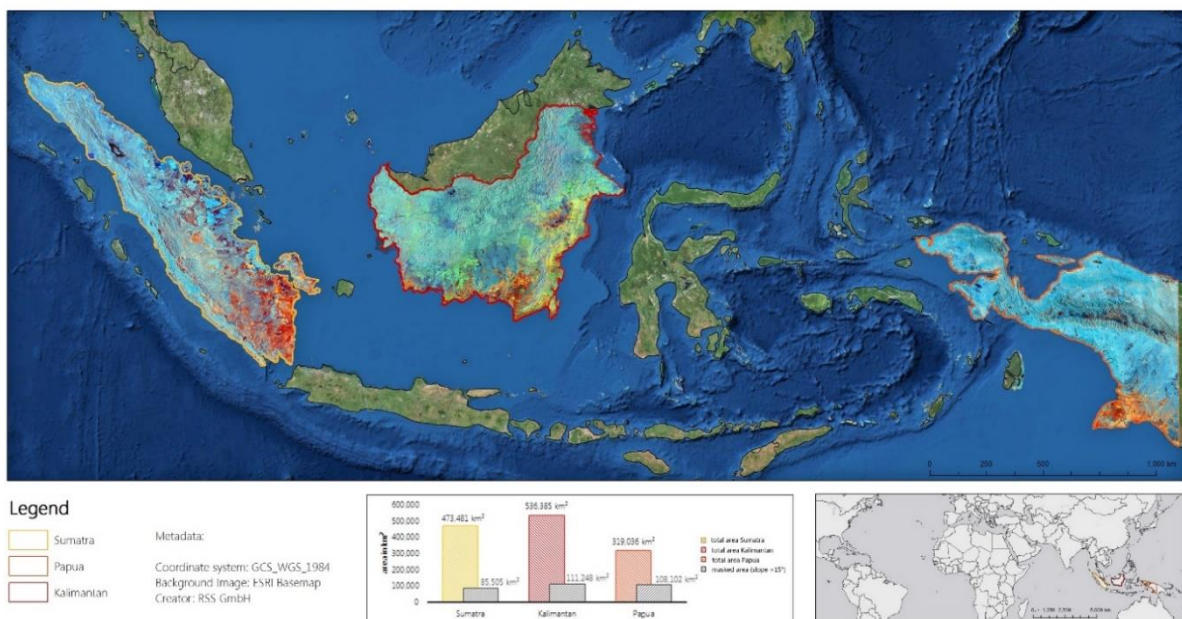


Figure 2: The project area covering Sumatra, Kalimantan and Papua. The bar chart depicts the total area of each region with excluded areas (slope > 15°).

Table 1: Number of MODIS Hotspots in the three regions between 01.07.2015 and 31.10.2015 and the fractional number of hotspots falling within slopes >15°.

	<b>Number of all hotspots</b>	<b>Number of hotspots in slopes &gt; 15°</b>	<b>Percentage of hotspots in slopes &gt; 15°</b>
<b>Sumatra</b>	51,749	802	1.55%
<b>Kalimantan</b>	41,897	774	1.85%
<b>Papua</b>	12,654	283	2.24%
<b>TOTAL</b>	106,300	1,859	1.75%

## 4 Datasets

### 4.1 Burned area detection

#### 4.1.1 Sentinel-1

Sentinel-1 is a two SAR satellite constellation carried out by the European Space Agency (ESA) operating at a centre frequency of 5.405 GHz. Sentinel-1A was launched in April 2014 and Sentinel-1B was launched in April 2016. The Interferometric Wide Swath (IW) is the primary operational mode over land and was used for this study. It acquires data with a 250 km swath at 5 m by 20 m spatial resolution. Ground Range Detected (GRD) Level-1 data with mid swath incidence angles between 38.85° and 39.26° were used in VV+VH polarization over Borneo and in VV polarization over Sumatra and Papua. The spatial resolution of the selected data is 10 m. Table 2 and Figure 3 provide an overview of Sentinel-1 data used for burned area mapping of 2015. A multi-month period was targeted for burned area assessment due to the difficulty of full coverage data availability with similar conditions. Since Sentinel-1B became operational in 2016, higher temporal resolution is available for future burned area assessments.

Table 2: Sentinel-1A data used for burned area mapping of 2015 showing the different characteristics (polarization, orbit and acquisition dates).

<b>Area</b>	<b>Polarization</b>	<b>Relative Orbit</b>	<b>Internal Orbit number (Figure 3)</b>	<b>Pass</b>	<b>Pre-fire acquisition</b>	<b>Post-fire acquisition</b>
Kalimantan	VV/VH	149	1	descending	06.07.2015	03.11.2015
Kalimantan	VV/VH	76	2	descending	01.07.2015	05.10.2015
Kalimantan	VV/VH	3	3	descending	20.07.2015	24.10.2015
Kalimantan	VV/VH	105	4	descending	27.07.2015	31.10.2015
Kalimantan	VV/VH	32	5	descending	22.07.2015	26.10.2015
Papua	VV	97	1	ascending	03.07.2015	31.10.2015
Papua	VV	24	2	ascending	28.06.2015	19.11.2015
Papua	VV	126	3	ascending	05.07.2015	09.10.2015
Papua	VV	53	4	ascending	30.06.2015	28.10.2015
Papua	VV	155	5	ascending	07.07.2015	04.11.2015
Papua	VV	82	6	ascending	02.07.2015	30.10.2015
Sumatra	VV	41	1	ascending	24.05.2015	02.12.2015
Sumatra	VV	143	2	ascending	24.06.2015	28.09.2015
Sumatra	VV	70	3	ascending	19.06.2015	17.10.2015
Sumatra	VV	171	4	ascending	26.06.2015	24.10.2015
Sumatra	VV	98	5	ascending	15.07.2015	12.11.2015

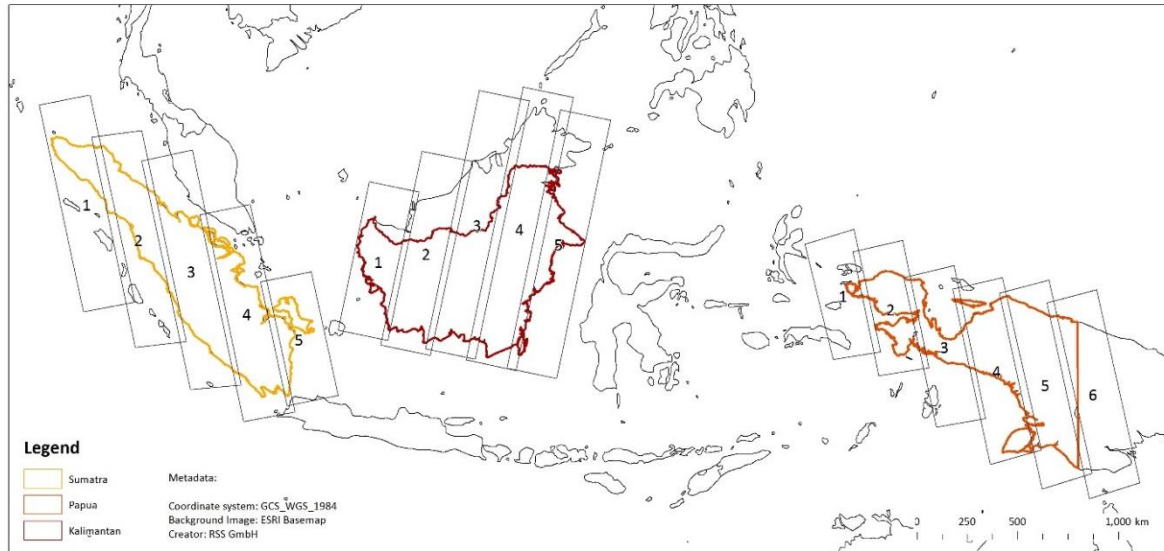


Figure 3: Overview of the different orbits for each region showing the internal orbit number listed in Table 2.

The selection process for the data was based on three criteria which needed to be met as well as possible (sorted by importance): data availability, fire season and precipitation (Figure 4).

**Data availability:** Different polarisations in different orbit directions are available for the three regions. Data were selected based on full-coverage availability with similar conditions for pre- and post-fire acquisitions with regard to orbit pass and polarization. In some cases the post-fire acquisitions are well before the end of the fire season (end of October). The reason for choosing data from end of September or beginning of October is mainly based on the availability of Sentinel-1 data in dry conditions.

**Fire season:** MODIS hotspot data (see 4.1.2) were analysed for fire season in order to choose Sentinel-1 images shortly before and right after the fire season in order to capture most of burned areas.

**Precipitation:** SAR backscatter is highly sensitive to water content of the surface due to its dielectric properties. Therefore, TRMM precipitation data (see 4.1.3) were incorporated into the data selection process in order to have dry and comparable conditions in pre- and post-fire acquisitions. If the designated dataset was acquired under wet conditions, another post-fire acquisition had to be selected which in some cases wasn't optimal regarding the coverage of the fire season (as also indicated by the dotted blue line in Figure 4).

The selection process of pre- and post-fire datasets is crucial regarding the result. Only burned areas which occur between the two time steps can be mapped. Therefore, this also has an impact on the emission estimations which are based on the burned area mapping. This approach estimates burned areas rather conservative.

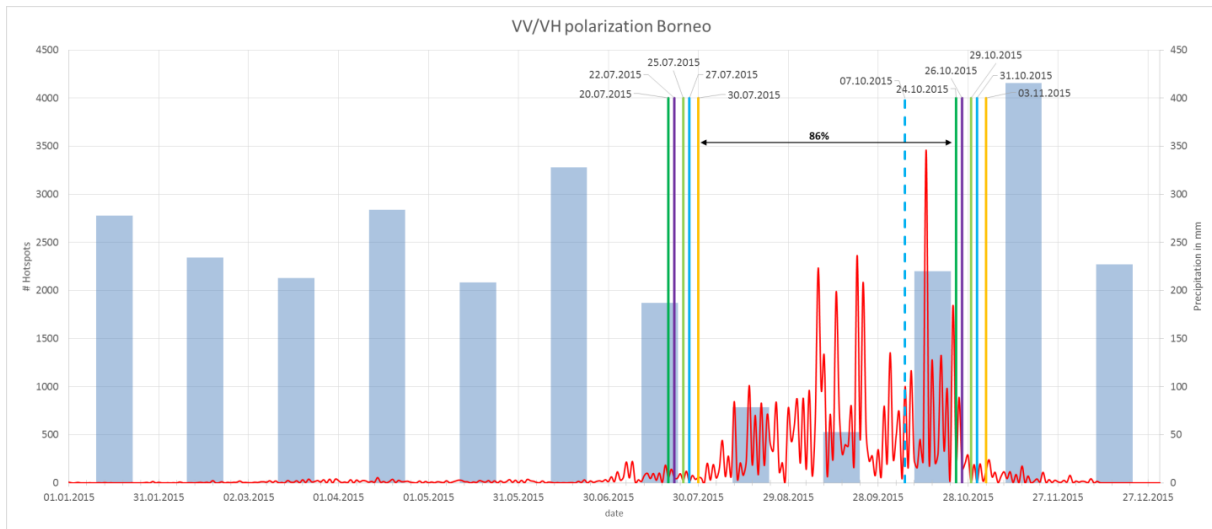


Figure 4: Available pre- and post-fire acquisitions (coloured bars) for the Kalimantan region are shown with monthly TRMM precipitation data (blue bars, right Y-Axis) and number of MODIS hotspots (red line, left Y-Axis).

#### 4.1.2 MODIS hotspots

The MODIS (Moderate Resolution Imaging Spectroradiometer) active fire product (Collection 6, MCD14ML) detects fires in 1 km<sup>2</sup> pixels that are burning at the time of overpass under relatively cloud-free conditions. The MODIS instrument is on board of NASA's Earth Observing System (EOS) Terra (EOS AM) and Aqua (EOS PM) satellites. A contextual algorithm is used where thresholds are first applied to the observed middle-infrared and thermal infrared brightness temperature and then false detections are rejected by examining the brightness temperature relative to neighbouring pixels [2].

#### 4.1.3 TRMM

For precipitation analysis the TRMM (Tropical Rainfall Measuring Mission) multi-satellite precipitation analysis product, also known as TRMM 3B42RT, was used [4], [5]. It provides precipitation data on a daily basis with a spatial resolution of 0.25°.

#### 4.1.4 SRTM

The SRTM provides a digital elevation model (DEM) from the Shuttle Radar Topography Mission (SRTM) flown in February 2000 which is available with a spatial resolution of 1 arc-second (approx. 30 m). The slope was calculated based on the SRTM for terrain analysis.

#### 4.1.5 PALSAR-2

The Advanced Land Observing Satellite-2 (ALOS-2) is a follow-on mission from the ALOS. The PALSAR-2 (Phased Array L-Band Synthetic Aperture Radar) on board ALOS-2 is an L-Band SAR sensor with a centre frequency of 1.2 GHz. ALOS-2 has a revisit time of 14 days. Data acquired in the ScanSAR mode (WBD) in HH and HV polarization (Level 1.5, Ceos format) were used in order to cross compare the developed burned area algorithm with L-Band SAR data on a subset area in Central Kalimantan. These images have a spatial resolution of 25 m.

#### 4.1.6 Water bodies

ESRI World Water Bodies provides a base map layer for lakes, oceans and large rivers and was used for delineating water bodies in order to exclude them for burned area classification. The vector file has a high spatial resolution especially regarding inland water streams and also includes intermittent water bodies which made this dataset highly valuable for excluding these error-prone areas.

#### 4.1.7 Sentinel-2

The Sentinel-2 mission consists of two identical satellites in the same orbit that cover the whole land surface, large islands, inland and coastal waters every five days at the equator. They carry wide swath high-resolution multispectral imagers with 13 spectral bands. Sentinel-2A was launched in June 2015 and Sentinel-2B is planned to be launched in April 2017. The spatial resolution ranges from 10 m to 60 m. Sentinel-2 was used for validation of the burned area product.

#### 4.1.8 Field data

In-situ GPS ground and aerial photos using drones were collected in collaboration with GIZ in South Sumatra in April 2016. GPS points in previously burned areas and non-burned areas were collected. Geo-located photos and aerial photos acquired by drones were also acquired in previously burned and non-burned areas. These data were used in order to validate the burned area product.

### 4.2 Fire Emission estimation

Total fire emission were calculated based on a combination of aboveground emissions from vegetation as well as peat emissions.

For the whole study area, aboveground emissions were estimated based on the MoEF (Ministry of Environment and Forestry) and the ESA CCI Land Cover classifications using emission factors from comprehensive LiDAR studies (GIZ FORCLIME and BIOCLIME projects, <http://www.forclime.org> and <http://www.bioclimate.org>). Emissions for Kalimantan region were also estimated with ESA's GlobBiomass (<http://globbiomass.org/>) regional AGB (aboveground biomass) map (see 4.2.1). In addition, a 100,000 km<sup>2</sup> area in Sumatra was classified for different forest types and used as reference for aboveground emission validation. Peat emissions were based on Wetlands International (WI) peat layer (see 4.2.5).

Table 3 provides an overview of used datasets for emission estimation.

Table 3: Used datasets for fire emission estimation.

product	Spatial resolution	Spatial coverage	Reference year	Data source
GlobBiomass	100 m	Kalimantan	2010	ALOS PALSAR mosaic
MoEF land cover	30 m	Project area	2013	Landsat
ESA CCI land cover	300 m	Project area	2010 (2008-2012)	MERIS
Reference land cover	30 m	100.000 km <sup>2</sup> in Sumatra	2014-2015	Landsat 8
WI peat layer	30 m	Project area	Sumatra: 1990-2002 Kalimantan: 2000-2002 Papua: 2000-2001	Landsat and field inventories

#### 4.2.1 ESA GlobBiomass map

The main purpose of the ESA DUE 'GlobBiomass' project is to better characterize and to reduce uncertainties of AGB estimates by developing an innovative synergistic mapping approach in five regional sites for the epochs 2005, 2010 and 2015 and for one global map for the year 2010. The regional map of Kalimantan containing AGB estimations at a spatial resolution of 100 m was used to estimate aboveground fire emissions and compare them to other approaches (for more information see <http://globbiomass.org/>).

#### 4.2.2 MoEF land cover

The Indonesian Ministry of Environment and Forestry (MoEF) provides land cover classification maps covering the time period 1990-2013 [6]. The maps are based on Landsat imagery and have a spatial resolution of 30 m. The most recent land cover map of 2013 was used for emission estimation because this is the closest to the classified burned area year (2015).

#### 4.2.3 ESA CCI land cover

The ESA CCI (Climate Change Initiative) land cover map is a 3-epoch series of global land cover maps at 300 m spatial resolution [7]. Each epoch covers a 5-year period: 1998-2002, 2003-2007, and 2008-2012. The maps were produced using a multi-year and multi-sensor strategy in order to make use of all suitable data and maximize product consistency. The most recent ESA cci land cover map of the reference year 2010 was used for fire emission estimation.

#### 4.2.4 Landsat-8

Landsat-8 (the successor of the Landsat-MSS, Landsat TM, Landsat ETM+ satellites) provides 30 m resolution multi-spectral imagery in 9 spectral bands ranging from VIS to SWIR. Also a panchromatic band with 15m resolutions is included. Landsat 8 data became available on May 30, 2013. Landsat-8 was used for land cover classification of the 100.000 km<sup>2</sup> reference site and for validation of the burned area product.

#### 4.2.5 SPOT-5

The SPOT-5 (Take5) experiments consist in using SPOT as a simulator of the image time series that ESA's Sentinel-2 mission will provide. One of the 150 SPOT-5 Take5 site are located inside the 100,000 km<sup>2</sup> reference site. One almost cloud free SPOT-5 Take5 image with a spatial resolution of 10 m was used for the reference land cover classification in order to increase cloud free areas because no cloud free Landsat-8 image for this area and time period exists.

#### 4.2.6 Wetlands International peat layer

The Wetlands International (WI) peat map is based on research conducted by Wahyunto et al. [8]–[10]. The resulting peat maps are based on interpretation of Landsat imagery and field inventories and were used in order to calculate peat emissions resulting from fire.

## 5 Methodology

### 5.1 Burned area detection

#### 5.1.1 Sentinel-1 processing

Sentinel-1 data were processed using the Sentinel-1 Toolbox implemented in SNAP (Sentinel Application Platform). All Senteinel-1 scenes were calibrated, radiometric corrected and speckle filtered (see Figure 5).

For processing the SNAP software provided by ESA including the Sentinel-1 toolbox was used to derive calibrated and corrected images. Before using the data, it is necessary to pre-process any radar satellite imagery by applying calibration, radiometric and geometric correction procedures as well as speckle

filter techniques. Pre-processing aims to get sensor independent backscatter values and a filtered image which shows reduced or no speckle noise. Only calibrated images can be sensibly compared regarding different sensors, acquisition times or different locations within one image [11].

The single tiles were first mosaicked and the multi-temporal SAR imagery were co-registered. SAR imagery were processed with normalized radar cross-section gamma-naught backscatter coefficients.

To reduce speckle in radar scenes, a multi-temporal speckle filter operator was applied [12]. This method obtains new images with reduced speckle effects from multi-temporal and multi-polarised images. It is based on the following relation:

$$J_k(x, y) = \frac{\langle I_k(x, y) \rangle}{N} \sum_{i=1}^N \frac{I_i(x, y)}{\langle I_i(x, y) \rangle} \text{ with } k = 1, \dots, N$$

Where  $J_k(x, y)$  is the radar intensity of the output image,  $k$  at pixel  $(x, y)$ ,  $I_i(x, y)$  is the radar intensity of the input image,  $i$  at pixel  $(x, y)$ ,  $\langle I_i(x, y) \rangle$  is the local average intensity of the input image  $i$  at pixel  $(x, y)$  and  $N$  is the number of images.

Different ratios were calculated based on the data input [13], [14]. For Borneo dual-pol (VV/VH) data was used, for Sumatra and Papua single-pol (VV) data. The usage of different Sentinel-1 data types (dual-pol data for Borneo and single-pol data for Sumatra and Papua) is based on the full coverage availability of the datasets for 2015 and the designated time period. A full single-pol Sentinel-1 pre- and post-fire coverage under dry conditions does not exist for Borneo as well as no full dual-polarised Sentinel-1 coverage under dry conditions does exist for Sumatra and Papua.

The ratios were used as input for segmentation to create objects, and served as features in the classification process. The following ratios were calculated where possible:

- $*R1 = \frac{VH_{t2}}{VH_{t1}}$
- $R2 = \frac{VV_{t2}}{VV_{t1}}$
- $R3 = VV_{t2} - VV_{t1}$
- $*R4 = VH_{t2} - VH_{t1}$
- $*R5 = R3 + R4$
- $*R6 = \frac{R1}{R2}$

\* only calculated for dual-pol (VV/VH) data (Kalimantan)

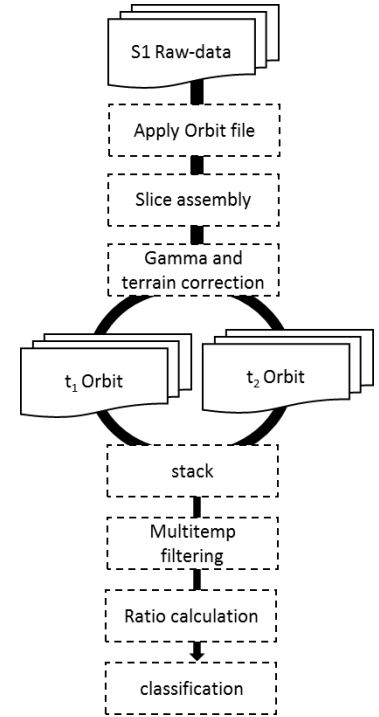


Figure 5: Pre-processing workflow.

where VV and VH are the polarizations, t1 is pre-fire and t2 post-fire Sentinel-1 acquisition. All available ratios were used for segmentation process. For burned area classification mainly the original backscatter layers and the difference ratios (R3, R4, R5) were used. The usage of single-pol or dual-pol Sentinel-1 data for burned area assessment does not have an influence with regard to object delineation or final classification accuracy.

### 5.1.2 Sentinel-2 and Landsat-8 pre-processing

The first step of the pre-processing is the geometric correction of the images. A geometric correction including orthorectification was carried out (if necessary). In order to apply terrain rectification, the SRTM was used. Geometric accuracy is expected to be below 0.5 pixels of the reference data.

The second step of the pre-processing is the removal of atmospheric distortions (scattering, illumination effects, adjacency effects), induced by water vapour and aerosols in the atmosphere, seasonally different illumination angles etc. An atmospheric correction was applied to each image using the software ATCOR [15]. This pre-processing step leads to a calibration of the data into an estimation of the surface reflectance without atmospheric distortion effects including topographic normalization. This calibration method facilitates a better scene-to-scene comparability of the radiometric measurements, which is a necessary precondition for the semi-automatic segment-based rule-set classification method applied in this study.

### 5.1.3 Object based burned area classification approach

For the object-based image analysis approach the software eCognition was used for segmentation and classification of burned areas. First so called "objects" or "segments" need to be generated which are then classified. Bottom up multi-resolution segmentation was used to create meaningful objects with respect to object size and delineation of burned areas. As input for the segmentation t1 and t2 backscatter layers were used as well as the calculated ratios.

After the segmentation the objects can be classified based on multiple features such as "mean VV value" or "mean 00\_vh\_ratio\_t2\_t1" (object based or pixel based) as well as relational features including neighbourhood features and hierarchical features. For the classification the before mentioned ratios were used based on fuzzy logic, which results in each object having a certain probability in belonging to the class burned area. In a final step the classification and objects were refined via applying "find enclosed by", "relations to neighbours", "pixel-based resizing" and other methods to improve classification and therefore increase accuracy. This approach assumes that changes in backscatter are caused by fires, whereas changes could have multiple other sources. Water bodies were excluded from burned area mapping in order to avoid misclassifications.

### 5.1.4 ALOS-2 cross comparison

A cross comparison between ALOS-2 PALSAR-2 and Sentinel-1 imagery with regard to burned area classification was done for a test site in Kalimantan. The pre- and post-fire image acquisitions are as close as possible to the Sentinel-1 image acquisitions (Table 4). The cross comparison was done in order to investigate the performance of different wavelengths (L-band for ALOS-2 and C-band for Sentinel-1) on burned area assessment.

*Table 4: Acquisition dates for Sentinel-1 and PALSAR-2 cross comparison.*

	<b>Pre-fire acquisition date</b>	<b>Post-fire acquisition date</b>
Sentinel-1	27/07/2015	31/10/2015
PALSAR-2	24/07/2015	21/10/2015

The same pre-processing and classification approach used for Sentinel-1 was also applied for PALSAR-2. However, the thresholds for burned area classification needed to be adjusted because the backscatter values of different acquisitions differed greatly due to climatic influences.

## 5.2 Reference land cover classification

The reference land cover classification was conducted in a site in South Sumatra which was defined in coordination with existing in-situ data and other project activities in Sumatra within the GIZ BIOCLIME project area and has a spatial extent of approximately 100,000 km<sup>2</sup> (Figure 6). The reference land cover classification was classified for different forest types based on pre-fire Landsat data (and for a small area Spot-5) of 2015 (and 2014 after the fire season) in order to validate vegetation fire emissions from existing land cover maps (e.g. MoEF and ESA CCI land cover).

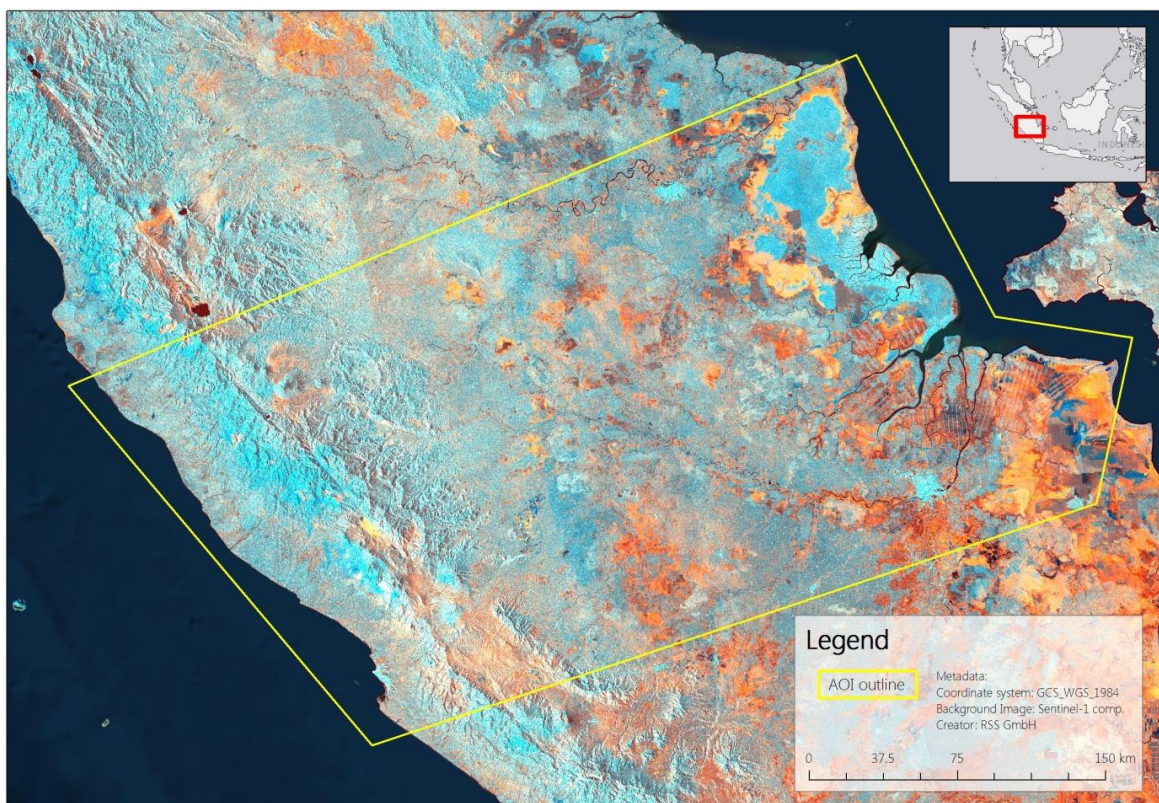


Figure 6: Location of the 100.000 km<sup>2</sup> site where the reference land cover classification was conducted.

The land cover classification was done with the Software eCognition which uses an object based image classification method. The first step of the classification process is the image segmentation, which accumulates spatially adjacent pixels with similar spectral properties into image objects. A threshold-based classification rule-set was then used to assign the land cover classes shown below to the image objects. Eventually, a visual screening of the classification results was conducted in order to reduce misclassifications and improve classification accuracy. The land cover classes follow the classification scheme suggested by IPCC [16] with slightly modifications with regard to the different carbon storage:

- Water
- Bare area/Non-vegetation
- Non-Forest (shrub, grassland, etc.)
- Plantations
- Forest further subdivided into

- Mangroves
- Peat swamp forests (based on the Wetlands International peat layer [17])
- Lowland forest (<300 m a.s.l. identified with the SRTM)
- Hill- and sub-montane forest (300-900 m a.s.l. identified with the SRTM)
- Lower montane forest (900-1500 m a.s.l. identified with the SRTM)
- Upper montane forest (>1500 m a.s.l. identified with the SRTM)

### 5.3 Emission estimation

Fire emission estimations are based on the intersection of the classified burned area layer and different land cover classifications or Aboveground Biomass (AGB) maps for vegetation fire emissions and peat map for assessing peat emissions from fire. Using different land cover classifications results in different fire emission estimates. These approaches and datasets are described below.

#### 5.3.1 Vegetation fire emissions

Two different approaches were used to calculate vegetation fire emissions: (a) using continuous AGB estimations (*continuous approach*) and (b) using land cover maps in combination with emission factors (*stratify and multiply approach*). A combustion efficiency of 1.0 was assumed, representing a simplified assumption based on complete combustion of the organic carbon. Introducing another combustion factor, such as 0.92 [18], would again represent a simplification and, in all likelihood, unique combustion factors should be used for different land cover types and fire intensities, which was beyond the scope of the present study.

Vegetation fire emissions estimated with the *continuous approach* were intersected with the AGB map of Kalimantan (see Figure 7). The burned biomass was converted to carbon dioxide equivalents (CO<sub>2</sub>-eq) assuming a carbon content of 50% in AGB [19]. The fraction of carbon in carbon dioxide is the ratio of their weights. The atomic weight of carbon is 12 atomic mass units, while the weight of carbon dioxide is 44, because it includes two oxygen atoms that each weigh 16. So, to switch from one to the other, use the formula: One ton of carbon equals  $44/12 = 11/3 = 3.67$  tons of carbon dioxide.

Emissions using the *stratify and multiply approach* were estimated by intersection of classified burned areas with MoEF and ESA CCI land cover maps, respectively. The *stratify and multiply approach* intersects the burned area with a land cover classification (where emission factors are assigned to each class) (see Figure 7). Based on the intersected area per land cover classes and the emission factors, total emissions for vegetation burning are calculated. In addition, the reference land cover classification covering 100,000 km<sup>2</sup> was classified for different forest types based on Landsat data (see 5.2) in order to validate vegetation fire emissions from land cover maps.

### Stratify and multiply approach



### Continuous approach

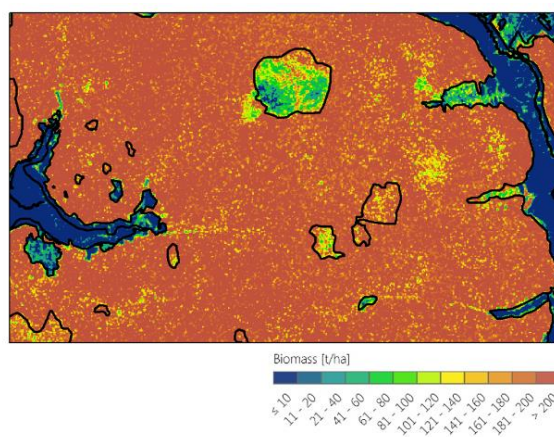


Figure 7: The left image represents the stratify and multiply approach, where a land cover classification with assigned emission factors is used to calculate emissions of burned areas. On the right the continuous approach is depicted, where each pixel holds different emission factors based on the biomass of the vegetation.

Regional emission factors determined within extensive LiDAR studies of the GIZ FORCLIME (<http://www.forclime.org/>) and BIOCLIME (<http://www.bioclimate.org/>) project were assigned to each of the land cover class and converted to CO<sub>2</sub>-eq as described above. Table 5 depicts a summary of the different land cover classes and emission factors used.

Table 5: Emission factors used for each land cover class for the different land cover classifications. The values are based on extensive LiDAR analyses conducted within the GIZ FORCLIME and BIOCLIME projects.

Land cover classification	Class name	AGB (t/ha)	CO <sub>2</sub> -eq (t/ha)
MoEF	Primary Dry Land Forest	545	1000
	Secondary Dry Land Forest	256	469
	Primary Mangrove Forest	198	364
	Primary Swamp Forest	235	431
	Secondary Mangrove Forest	44	82
	Secondary Swamp Forest	127	233
	HTI	90	165
	Plantation	69	127
	Housing	0	0
	Savannah	25	46
	Scrubland	25	46
	Swamp Scrubland	77	141
	Swamp	12	22
	Dry Rice Land	10	18
	Dry Rice Land Mixed w/Scrub	95	18
	Rice Land	10	18
	Fish Pond	0	0
	Bare Land	0	0
	Mining	0	0
	Transmigration	0	0

	Airport	0	0
	Bodies of Water	0	0
<i>ESA CCI</i>	Tree cover, broadleaved, evergreen, closed to open (>15%)	337	618
	Tree cover, flooded, fresh or brakish water	201	369
	Tree cover, flooded, saline water	185	339
	Mosaic natural vegetation (tree, shrub, herbaceous cover) (>50%) / cropland (<50%)	105	193
	Mosaic cropland (>50%) / natural vegetation (tree, shrub, herbaceous cover) (<50%)	60	110
	Mosaic tree and shrub (>50%) / herbaceous cover (<50%)	40	73
	Cropland, rainfed	31	58
	Herbaceous cover	31	58
	Tree or shrub cover	31	58
	Shrubland	25	46
	Shrubland evergreen	25	46
	Shrubland deciduous	25	46
	Sparse vegetation (tree, shrub, herbaceous cover) (<15%)	25	46
	Sparse shrub (<15%)	25	46
	Sparse herbaceous cover (<15%)	25	46
	Cropland, irrigated or post-flooding	10	18
	Shrub or herbaceous cover, flooded, fresh/saline/brakish water	10	18
	Grassland	6	11
	No data	0	0
	Urban areas	0	0
	Bare areas	0	0
	Consolidated bare areas	0	0
	Unconsolidated bare areas	0	0
	Water bodies	0	0
<i>Reference 100,000 km<sup>2</sup></i>	Lowland forest (<300m a.s.l. identified with the SRTM)	166	305
	Lower montane forest (900-1500m a.s.l. identified with the SRTM)	347	637
	Hill- and sub-montane forest (300-900m a.s.l. identified with the SRTM)	264	484
	Upper montane forest (>1500m a.s.l. identified with the SRTM)	248	455
	Peat swamp forests (based on the Wetlands International peat layer [9])	201	369
	Mangroves	185	339
	Plantations	69	127
	Non-Forest (shrub, grassland, etc.)	25	46
	water	0	0
	Bare area/Non-vegetation	0	0

### 5.3.2 Peat fire emissions

Peat stores huge amounts of Carbon and therefore leads to large emissions when burned. To calculate these emissions we used the approach suggested by Konecny et al. [20]. A discrimination between the first and second or more fires is made with regard to the burn depth into the peat and the amount of carbon released.

Peat fire emissions were calculated by intersecting the classified burned areas, land cover or AGB maps and peat layers assuming that forest land cover classes on peat burn the first time and all other land cover classes (scrubland, grassland, swamp, etc.) experience at least the second fire. Using the AGB estimation map, we assumed that areas with AGB higher than 100 t/ha burn for the first time while areas with lower biomass values have already been burned. The approach suggested by Konecny et al. [20] determines a peat burn depth of 17 cm for the first fire, and the average burn depth for the second and third fire, 8 cm, was used for two or more fires. Consequently, a carbon loss values of 114 tC/ha and 51 tC/ha was applied for the first and more than one fire, respectively. The carbon loss was converted to CO<sub>2</sub>-eq with the factor 3.67 (see above).

## 5.4 Strengths, limitations and weakness of the developed approach

An important advantage of the SAR system is the daylight and weather independence as the signal can penetrate through clouds, haze and smoke. This is especially important in the tropical region which is often obscured by clouds. However, using SAR Radar backscatter for detecting burned areas comes along with some specific challenges and limitations. The known limitations of SAR are mainly related to steep terrain. These effects are inevitable and need to be taken into account in the classification and analysis of the data. Applying terrain correction reduces these effects, but do not eliminate them. Therefore, areas with a slope >15° were excluded for burned area mapping.

The selection of Sentinel-1 scenes for processing is crucial and described in 4.1.1. Moisture and heavy rainfall influences the SAR signal and may lead to errors in burned area classifications.

The developed approach for burned area classification does not only map burned area but rather areas with reduced backscatter below a certain threshold. It is assumed that the major share of backscatter reductions during the dry season results from fires as it is often used as a cheap tool to clear large-scale areas (slash and burn). In general, backscatter reduction might also result from inundation (which is partly excluded with the water layer), rapid change in agricultural areas or logging, for example.

A multi-temporal Sentinel-1 dataset might help to overcome some of these error sources. However, it was not possible to use a multi-temporal Sentinel-1 dataset for 2015 due to data availability having only Sentinel-1A. With Sentinel-1B in space, the possibility of using a multi-temporal dataset for the 2016 burned area assessment increases.

## 6 Products

The final products include burned area maps, pre-fire land cover classification and related carbon dioxide emissions for Sumatra, Kalimantan and West-Papua for the years 2015 and 2016, respectively and are included in the PVR.

## 7 References

- [1] GFED, "Global Fire Emission Database," 2015. [Online]. Available: <http://www.globalfiredata.org/updates.html>.
- [2] L. Giglio, J. Descloitres, C. O. Justice, and Y. J. Kaufman, "An Enhanced Contextual Fire Detection Algorithm

- for MODIS," *Remote Sens. Environ.*, vol. 87, no. 2–3, pp. 273–282, Oct. 2003.
- [3] A. E. Melchiori, A. W. Setzer, F. Morelli, R. Libonati, P. de A. Cândido, and S. C. de Jesús, "A Landsat-TM/OLI algorithm for burned areas in the Brazilian Cerrado: preliminary results," in *Advances in forest fire research.*, Coimbra, 2014, p. 30.
- [4] G. J. Huffman, R. F. Adler, D. T. Bolvin, and E. J. Nelkin, "The TRMM Multi-Satellite Precipitation Analysis (TMPA)," in *Satellite Rainfall Applications for Surface Hydrology*, Dordrecht: Springer Netherlands, 2010, pp. 3–22.
- [5] G. J. Huffman, D. T. Bolvin, E. J. Nelkin, D. B. Wolff, R. F. Adler, G. Gu, Y. Hong, K. P. Bowman, and E. F. Stocker, "The TRMM Multisatellite Precipitation Analysis (TMPA): Quasi-Global, Multiyear, Combined-Sensor Precipitation Estimates at Fine Scales," *J. Hydrometeorol.*, vol. 8, no. 1, pp. 38–55, Feb. 2007.
- [6] "Greenpeace," 2016. [Online]. Available: <http://www.greenpeace.org/seasia/id/Global/seasia/Indonesia/Code/>.
- [7] ESA, "CCI land cover." [Online]. Available: <http://www.esa-landcover-cci.org/>.
- [8] S. R. Wahyunto and H. Subagjo, "Peta Luas Sebaran Lahan Gambut dan Kandungan Kargon di Pulau Sumatera," *Bogor, Indones. Wetl. Int. Indones. Progr. Rapid Assess. Tripa Batang Toru-117-Wildlife Habitat Canada*, 2003.
- [9] R. S. Wahyunto and H. Subagjo, "Peta Sebaran Lahan Gambut, Luas dan Kandungan Karbon di Kalimantan/Map of Peatland Distribution Area and Carbon Content in Kalimantan," *Wetl. Int. Indones. Program. Wildl. Habitat Canada, Bogor, Indones.*, 2004.
- [10] B. H. Wahyunto, Hasyim Bekti, and Fitri Widiastuti, "Peta Sebaran Lahan Gambut, Luas dan Kandungan Karbon di Papua/Maps of Peatland Distribution, Area and Carbon Content in Papua," *Wetl. Int. Program. Wildl. Habitat Canada*, 2006.
- [11] C. Oliver and S. Quegan, *Understanding Synthetic Aperture Radar Images*. 2004.
- [12] S. Quegan, T. Le Toan, J. J. Yu, F. Ribbes, and N. Floury, "Multitemporal ERS SAR analysis applied to forest mapping," *IEEE Trans. Geosci. Remote Sens.*, vol. 38, no. 2, pp. 741–753, Mar. 2000.
- [13] R. B. Thapa, M. Watanabe, T. Motohka, and M. Shimada, "Potential of high-resolution ALOS-PALSAR mosaic texture for aboveground forest carbon tracking in tropical region," *Remote Sens. Environ.*, vol. 160, pp. 122–133, Apr. 2015.
- [14] O. Hamdan, H. Khali Aziz, and I. Mohd Hasmadi, "L-band ALOS PALSAR for biomass estimation of Matang Mangroves, Malaysia," *Remote Sens. Environ.*, vol. 155, pp. 69–78, Dec. 2014.
- [15] R. Richter and D. Schläper, "Atmospheric / Topographic Correction for Satellite Imagery." ATCOR-2/3 User Guide, Version 8.3.1, [http://www.rese.ch/pdf/atcor3\\_manual.pdf](http://www.rese.ch/pdf/atcor3_manual.pdf), pp. 1–238, 2014.
- [16] IPCC, *IPCC Guidelines for National Greenhouse Gas Inventories. Prepared by the National Greenhouse Gas Inventories Programme*. Eggleston, H.S., Buendia, L., Miwa, k., Ngara, T. and Tanabe, K.(Eds).Published: IGES, Japan, 2006.
- [17] W. International, "Peatlands." [Online]. Available: <http://www.wetlands.org/Whatarewetlands/Peatlands/tabid/2737/Default.aspx>.
- [18] S. Enghart, J. Jubanski, and F. Siegert, "Quantifying Dynamics in Tropical Peat Swamp Forest Biomass with Multi-Temporal LiDAR Datasets," *Remote Sens.*, vol. 5, no. 5, pp. 2368–2388, May 2013.
- [19] S. J. Goetz, A. Baccini, N. Laporte, T. Johns, W. Walker, J. Kellndorfer, R. A. Houghton, and M. Sun, "Mapping and monitoring carbon stocks with satellite observations: a comparison of methods.," *Carbon Balance Manag.*, vol. 4, no. 1, p. 2, Jan. 2009.
- [20] K. Konecny, U. Ballhorn, P. Navratil, J. Jubanski, S. E. Page, K. Tansey, A. Hooijer, R. Vernimmen, and F. Siegert, "Variable carbon losses from recurrent fires in drained tropical peatlands.," *Glob. Chang. Biol.*, Dec. 2015.